The 2nd International Conference on Multidisciplinary Engineering and Applied Sciences (ICMEAS-2023)

Enhancing Perovskite Film Properties Through Solvent Annealing Techniques

Dahiru M. Sanni
Faculty of Science.
Nile University of Nigeria
Abuja, Nigeria
dahirusanni@gmail.com

Abdulhakeem Bello
Department of Physics
African University of Science and Technology
Abuja, Nigeria
abello@aust.edu.ng

Sharafadeen A. Adeniji
Department of Physics
Faculty of Science
Nile University of Nigeria
Abuja, Nigeria
adeniji.sharafadeen@nileuniversity.edu.ng

Richard K. Koech
Department of Mathematics, Physics and Computing
Moi University
Eldoret, Kenya
rkkoech09@gmail.com

Uchenna C. Obi
Department of Materials Science and Engineering
African University of Science and Technology
Abuja, Nigeria
uobi@aust.edu.ng

Omolara V. Oyelade
Department of Physics, Bingham University, Karu Nasarawa State, Nigeria oyeladeov@binghamuni.edu.ng

2023 2nd International Conference on Multidisciplinary Engineering and Applied Science (ICMEAS) | 979-8-3503-5883-4/23/$31.00 ©2023 IEEE | DOI: 10.1109/ICMEAS58693.2023.10379265

Abstract*— In this study, we investigated how solvent annealing affected the material properties of perovskite films derived from precursors of dehydrated Pb-acetate. The perovskite active layer was produced by depositing the perovskite solution using a one-step spin-coating method, followed by either 5 minutes of solvent annealing in DMF or IPA vapour or 5 minutes of thermal annealing on a hotplate at a temperature of 90 °C. Thermal annealing (TA), annealing in DMF vapour, and annealing in IPA vapour were used to form the perovskite active layers. The perovskite films made from IPA vapou show the best material properties, and the perovskite films obtained from the thermal annealing process have the poorest material properties. Our research showed that perovskite films produced using solvent engineering methods have better film properties.

Keywords— ***Solvent annealing, perovskite films, material properties, lead acetate***

I. Introduction

Power conversion efficiency (PCE) of lead halide perovskite solar cells (PSCs) has greatly improved over the past ten years, rising from 3.8% in 2009 to a record-high 25.2% at this time [1]. The outstanding advantages of the perovskite, such as their high absorption coefficient, variable bandgap, long diffusion length, fast solution processing, low excitation binding energy, etc. [2]. Mesoporous TiO_2 scaffolds and planer heterojunction designs, among other device topologies, are made possible by the unique advantages of perovskite materials [3]. A planar design can be described by either the traditional (n-i-p) or (p-i-n) structures. Planar architecture has a basic structure and a low processing temperature below 100 ^oC, in contrast to mesoporous architecture, which has a complex cell structure and a higher processing temperature exceeding 450 ^oC [4]. Researchers studying PSCs are beginning to favour the p-i-n architecture because of the absence of hysteresis during the J-V measurement and the processing temperature is low [5]. Because the p-i-n architecture can be fabricated at low temperatures, flexible substrates and a wide range of functional materials can benefit from it [6].

The PSCs were made using a variety of deposition techniques, including, 1-step spin coating, 2-step sequential deposition, dip coating, spray coating, vapour deposition, vapour-aided solution deposition, and blade coating methods [7]. The CH3NH3PbI3 methylammonium lead halide PSCs were produced using a range of precursor substances. It is feasible to produce $CH_3NH_3PbI_3$ by combining lead iodide (PbI_2) and methylammonium iodide (MAI) in a 1:1 solution. Additionally, by reacting MAI with different non-halides of lead, such as "lead acetate ($Pb(OAc)_2$)", "lead nitrate ($Pb(NO_3)$), and lead (II) acetylacetonate ($Pb(acac)_2$)", $CH_3NH_3PbI_3$ can be created. [8]. PSCs have advanced well when Pb $(OAc)_2$ is utilised as the Pb source.[9]. The PSCs generated from $Pb(OAc)_2$ have the advantage of speeding up the crystal growth of $CH_3NH_3PbI_3$, which in turn often generates smooth perovskite films with fewer pinholes due to how easily the N-methylammonium acetate CH_3NH_3COO was removed. As a result of the fast crystal growth process, which produces more defect sites and grain boundaries, the perovskite films frequently have smaller grains. Solvent annealing is one technique for improving the grain sizes and quality of the perovskite layer. Numerous studies have improved the perovskite film quality using solvent engineering techniques [10]. Precursors based on lead halide are used in the majority of these works. However, J. Qing et al. report that solvent annealing can raise the PCE of PSCs produced from lead acetate from 10.11% to 12.7% in DMF vapour [11].

This study employs a 1-step deposition method for attaching the perovskite layer before annealing. We used both solvent annealing and thermal annealing (TA) techniques to make the perovskite layer. As part of the solvent annealing process, we annealed the perovskite films in the DMF and IPA vapour for 5 minutes.

II. Experimental Procedure

A. Materials

The "phenyl-C61-butyric acid methyl ester (PCBM)", poly (3,4-ethylene dioxythiophene), and poly (styrene sulfonate were all supplied by Ossila and used without further purification. Dimethylformamide (DMF), isopropyl alcohol (IPA), and lead acetate trihydrate ($PbAc_2.3H_2O$) were all provided by Alfa Aesar. The "lead acetate trihydrate ($PbAc_2.3H_2O$)" was subsequently processed to produce the "dehydrated lead acetate ($Pb(Ac)_2$)" by dehydrating it in a flowing nitrogen gas for a protracted period of time at a temperature of 80 ^oC.

B. Film Formation and Materials Characterisation

The glass/ITO substrates were cleaned in an ultrasonic bath for 16 minutes in detergent solution, deionized water, acetone, and IPA, respectively, before being dried with flowing nitrogen gas. The glass and ITO were then exposed for 17 minutes to an ultraviolet-ozone (UVO) atmosphere. The substrate has a 0.2 cm2 active surface and measures 2.5 cm by 2.5 cm. After the PEDOT:PSS was deposited on the glass/ITO substrate at a rate of 4 x 10^3 revolution per minute for one minute, the hole transport layer (HTL) was created by TA on a hot plate at a temperature of 150 ºC for 16 minutes. The perovskite solution was made by dissolving 3.0 mmol of MAI and 1.0 mmol of $Pb(Ac)_2$ in 1 mL of DMF.

The active layer was synthesised by depositing the solution on the PEDOT:PSS at a speed of 4 x 10^3 revolution per minute for 1 minute, before the TA or solvent annealing. The three sets of samples are labelled as follows: TA for samples from the thermal annealing process; DMF and IPA for samples from the DMF and IPA vapour annealing processes. The samples were put on the hotplate at 90 ºC for the DMF vapour annealing process. About 10 µL of DMF was added, and then the samples were covered with a petri dish. The samples were heated for five minutes in a DMF vapour atmosphere. For the IPA vapour annealing, the same procedure was followed; 10 µL of IPA were dropped on the hotplate next to the samples and were covered with glass petri dishes. In an IPA vapour environment, the samples underwent a 5-minute annealing process. The samples were immediately placed on the hotplate for five minutes at a temperature of 90 ºC for the TA after being deposited. The schematic diagram for producing a perovskite film utilising the TA and vapour annealing methods are shown in Figures 1(a) and (b). These sets of samples were met for scanning electron microscopy (SEM). The samples prepared for XRD, UV and PL were deposited directly on the treated plain glass without PEDOT:PSS.

"SEM-XL30 Environmental FEG (FEI)" was used to measure the morphology of the perovskite films in their as-prepared state. By producing the Copper K radiation at an anode tension of 40 kV and a filament current of 45 mA, X-ray diffraction (XRD) was used to analyse the perovskite crystal formation. For the evaluation, a step-size of 0.01 degrees was applied. The Cary 5000 UV/VIS photo spectrometer was used to characterise the absorption spectra. A femtosecond Ti:S laser (Spectra-Physics) with a frequency doubler and a pulse selection was used to measure the Photoluminescence (PL) decay time for the samples as-prepared at 775 nm. At 425 nm, the excitation wavelength was set.

III. RESULTS AND DISCUSSION

The perovskite solution was deposited on a PDOT:PSS/ITO/GLASS substrate a speed of 4 x 10^3 revolution per minute for one minute before thermal annealing on a hotplate and solvent annealing in DMF and IPA vapours to form three different perovskite films for SEM characterization. Figure 2a shows the SEM photographs of perovskite films obtained from the thermal annealing process; fig. 2b represents perovskite films obtained from solvent annealing in a DMF vapour; and fig. 2c shows the SEM morphology of perovskite films derived from IPA solvent annealing. From the SEM images, it is observed that the perovskite films obtained from the IPA vapour have better crystallinity and improved grain sizes, while samples obtained from the thermal annealing process have smaller grain sizes. The perovskite films derived from the DMF vapour have improved crystallinity in comparison to those obtained via the TA process. However, this set of samples is inferior compared to the samples obtained from IPA vapour. From the SEM characterization, it is observed that solvent annealing techniques generally improve the perovskite film quality. The improved film quality will benefit charge transport due to fewer pinholes and fewer boundary defects, which are sites for recombination. However, it is observed that the films obtained from DMF vapour are inferior compared to those obtained from IPA vapour. This could be due to the perovskite precursor layer's one-step solvent engineering deposition and the intermediate PbI2-MAI-DMF phases. These intermediary phases will change during the annealing procedure and emit DMF vapour. Since the formation of perovskites is a reversible reaction, increasing the amount of DMF used

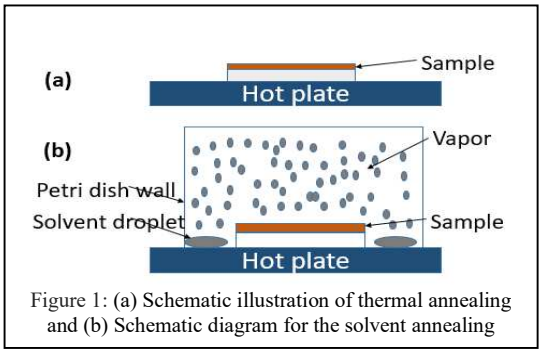

Figure 1: (a) Schematic illustration of thermal annealing and (b) Schematic diagram for the solvent annealing

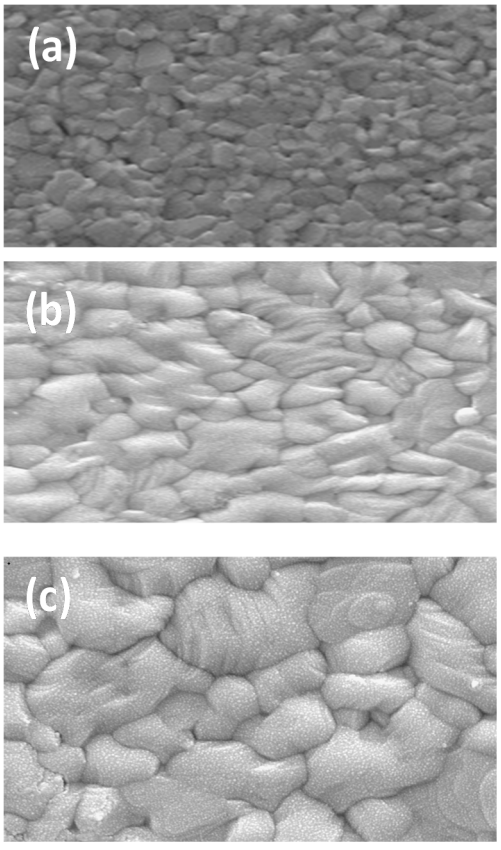

Figure 2: SEM Photographs of perovskite films obtained via (a) TA (b) DMF vapour annealing, and (c) IPA vapour annealing processes

979-8-3503-5883-4/23/$31.00 ©2023 IEEE

during annealing will produce too much DMF vapour and prevent CH3NH3PbI3 from recrystallizing.

The XRD peaks of the perovskite layer produced by TA, DMF vapour, and IPA vapour annealing are presented in figure 3(a). The samples made by TA, DMF solvent annealing, and IPA solvent annealing exhibit clear diffraction peaks at 14.19 and 28.42, which are associated with the peak (110) and (220) lattice planes of the $CH_3NH_3PbI_3$ phase, respectively, according to the XRD study. The samples made with DMF vapour annealing exhibit the next-highest peak intensities after the perovskite films made from IPA vapour. The intensity is lowest in the sample that was produced using TA. The SEM images corroborate the findings of the XRD patterns by revealing that the film produced using IPA vapor exhibits the highest peak intensity in the XRD results. Additionally, the SEM analysis indicates that films created through IPA vapor deposition display superior film quality, whereas those produced with TA exhibit the lowest XRD peak intensity and the poorest film quality among all the samples.

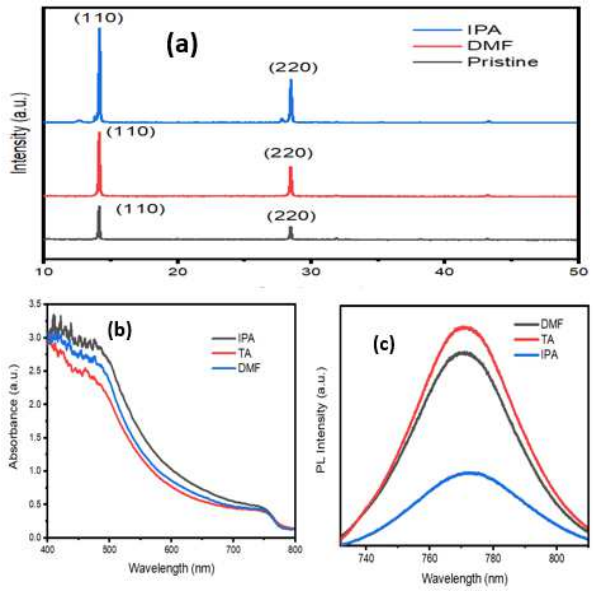

Figure 3: (a) XRD patterns; (b) Absorption spectra; (c) Steady Photoluminescence spectra of perovskite films prepared from TA, DMF vapour annealing, and IPA solvent annealing

The UV-vis spectra of perovskite films created using the TA, DMF, and IPA solvent annealing techniques are displayed in Fig. 3(b). When compared to films prepared with TA and DMF, the film prepared with IPA slightly exhibits superior absorbance. This improved absorbance may be a consequence of improved film quality. Characterization of photoluminescence (PL) spectra is done to better understand how the different annealing processes affects the performance of the samples. No red-shift or blue-shift photoluminescence spectra are seen in the steady-state PL spectra of the perovskite film deposited on glass as shown in fig. 3c, this suggests that the bandgap of the perovskite films made from TA, DMF and IPA has not changed. The lower quality of the perovskite films as compared to the DMF and IPA-derived films results in a decrease in the intensity peak of films produced from TA, whereas the IPA-derived films have the highest intensity peak because more electrons are removed from the films.

IV. CONCLUSION

To improve the quality of films produced by the one-step deposition approach, we used a straightforward solvent annealing technique. We discovered that the visible light absorption and grain size of the perovskite layer were higher. This enhancement might be attributable to the solvent evaporating significantly more slowly, which is good for perovskite grain development. The solvent-annealed perovskite films have improved grain sizes and fewer pinholes, which will enhance charge collection in the perovskite films.

.

REFERENCES

[1] NREL, "Best Research-Cell Efficiencies, https://www.nrel.gov/pv/assets/pdfs/ best-research-cell-efficiencies.20190802.pdf," 2019. .

[2] S. D. Stranks *et al.*, "Electron-Hole Diffusion Lengths Exceeding 1 Micrometer in an Organometal Trihalide Perovskite Absorber," *Science (80-.).*, vol. 342, no. October, pp. 341–345, 2013.

[3] Y. Chen, A. Yerramilli, Y. Shen, Z. Zhao, and T. Alford, "Effect of excessive Pb content in the precursor solutions on the properties of the lead acetate derived CH3NH3PbI3 perovskite solar cells," *Sol. Energy Mater. Sol. Cells*, vol. 174, no. June 2017, pp. 478–484, 2018.

[4] J. Burschka *et al.*, "Sequential deposition as a route to high-performance perovskite-sensitized solar cells," *Nature*, vol. 499, no. 18, pp. 316–319, 2013.

[5] A. S. Yerramilli, Y. Chen, D. Sanni, J. Asare, N. D. Theodore, and T. L. Alford, "Impact of excess lead on the stability and photo-induced degradation of lead halide perovskite solar cells," *Org. Electron. physics, Mater. Appl.*, vol. 59, pp. 107–112, 2018.

[6] J. Asare *et al.*, "A Hybrid Hole Transport Layer for Perovskite-Based Solar Cells," *energies*, pp. 1–13, 2021.

[7] D. Gedamu *et al.*, "Solvent-Antisolvent Ambient Processed Large Grain Size Perovskite Thin Films for High-Performance Solar Cells," *Sci. Rep.*, vol. 8, no. 1, pp. 1–11, 2018.

[8] M. Sima, E. Vasile, and M. Sima, "Lead acetate film as precursor for two-step deposition of CH 3 NH 3 PbI 3," *Mater. Res. Bull.*, vol. 89, pp. 89–96, 2017.

[9] D. M. Sanni *et al.*, "Impact of precursor concentration on the properties of perovskite solar cells obtained from the dehydrated lead acetate precursors *J. Vac. Sci. Technol. A*, vol. 032801, no. October 2021.

[10] J. Mou *et al.*, "Butanol-assisted solvent annealing of - CH3NH3PbI3 film for high- efficient perovskite solar cells," *J. Mater. Sci. Mater. Electron.*, vol. 30,

979-8-3503-5883-4/23/$31.00 ©2023 IEEE

no. 0, pp. 746–752, 2019.

[11] J. Qing *et al.*, "Simple fabrication of perovskite solar cells using lead acetate as lead source at low temperature," *Org. Electron. physics, Mater. Appl.*, vol. 27, pp. 12–17, 2015.

979-8-3503-5883-4/23/$31.00 ©2023 IEEE